Optimal Bidding Strategy for PV and BESSs in Joint Energy and Frequency Regulation Markets Considering Carbon Reduction Benefits

Jing Bian, Yuheng Song, Chen Ding, Jianing Cheng, Shiqiang Li, and Guoqing Li

***Abstract*—Photovoltaic (PV) and battery energy storage systems (BESSs) are key components in the energy market and crucial contributors to carbon emission reduction targets. These systems can not only provide energy but can also generate considerable revenue by providing frequency regulation services and participating in carbon trading. This study proposes a bidding strategy for PV and BESSs operating in joint energy and frequency regulation markets, with a specific focus on carbon reduction benefits. A two-stage bidding framework that optimizes the profit of PV and BESSs is presented. In the first stage, the day-ahead energy market takes into account potential real-time forecast deviations. In the second stage, the real-time balancing market uses a rolling optimization method to account for multiple uncertainties. Notably, a real-time frequency regulation control method is proposed for the participation of PV and BESSs in automatic generation control (AGC). This is particularly relevant given the uncertainty of grid frequency fluctuations in the optimization model of the real-time balancing market. This control method dynamically assigns the frequency regulation amount undertaken by the PV and BESSs according to the control interval in which the area control error (ACE) occurs. The case study results demonstrate that the proposed bidding strategy not only enables the PV and BESSs to effectively participate in the grid frequency regulation response but also yields considerable carbon emission reduction benefits and effectively improves the system operation economy.**

***Index Terms*—Photovoltaic (PV), battery energy storage system (BESS), energy market, carbon market, frequency regulation service, bidding strategy.**

I. Introduction

NEW energy generation, represented by photovoltaic (PV) power generation, is a green, low-carbon, and environmentally friendly solution that embodies low-carbon ideals. The sector has been developing at a rapid pace. However, considerable uncertainties in new energy generation, including PV power generation, pose some limitations to its growth in the electricity market [1].

Deploying battery energy storage systems (BESSs) for new energy sites has proven effective not only in eliminating fluctuations in new energy output [2] but also in improving grid frequency stability [3]. In recent years, PV and BESSs have gained widespread attention as pivotal operational models that can effectively improve the economic efficiency of PV power stations [4].

Previous studies have investigated the integration of new energy and BESSs in the electricity market. Reference [5] proposed a bidding strategy for PV and BESSs to participate in energy and frequency reserve markets. By employing model predictive control (MPC) methods to handle the uncertainty associated with PV output, the economic efficiency of PV and BESSs was enhanced. Reference [6] evaluated a potential business case for BESSs; in particular, it investigated the integration of market application and services into a PV-assisted fast-charging station for electric vehicles. Reference [7] developed a robust optimization model based on MPC, considering the uncertainties in new energy output and real-time electricity prices. This model was used for the joint operation of new energy power stations and BESSs. Reference [8] introduced optimal scheduling for an energy management system (EMS) model. This model was designed for a hydrogen production system integrated with the PV and BESSs. Advanced BESS life models were used in [9] and [10] to improve the BESS usage and boost the profitability of wind stations. Reference [11] proposed an approach to coordinating the optimization scale and control strategies for maximizing the revenue of PV and BESSs. This study used online MPC to offset PV prediction errors by participating in the intraday market.

With the continuous development of the carbon market, PV power stations can now participate in trading through China Certified Emission Reductions (CCERs) and reap benefits from carbon emission reductions in the carbon market. The optimization of new energy operations within the framework of carbon trading has been a focal point of many studies. For instance, [12] introduced a carbon trading mechanism into a collaborative bidding model for PV power generation systems and electric vehicles. This mechanism fully

Manuscript received: September 26, 2023; revised: December 26, 2023; accepted: February 1, 2024. Date of CrossCheck: February 1, 2024. Date of online publication: February 12, 2024.

This work was supported by the Jilin Province Science and Technology Development Plan Project (No. 20220203163SF).

J. Bian (corresponding author), Y. Song, J. Cheng, S. Li, and G. Li are with the Key Laboratory of Modern Power System Simulation and Control & Renewable Energy Technology Ministry of Education, Northeast Electric Power University, Jilin 132000, China (e-mail: bj_jjj@163.com; a911729743@163.com; 3127103457@qq.com; neepu_lsq@163.com; LGQ@mail.neepu.edu.cn).

C. Ding is with Datang Northeast Electric Power Test & Research Institute Co., Ltd., Changchun 130102, China (e-mail: dhdh1999@163.com).

DOI: 10.35833/MPCE.2023.000707

capitalized on the advantages of PV power generation and electric vehicles in terms of carbon emission reduction, achieving an energy–economic balance and fostering low-carbon systems. Reference [13] proposed a multi-objective optimization model, considering the cost of wind power reserves and conventional carbon trading. This model simultaneously considered energy–economic and low-carbon system objectives. However, most of the current studies on low-carbon power systems primarily focus on optimization scheduling on the generation side. Therefore, there is a need to further evaluate how carbon trading affects the bidding strategies of new energy bases.

In addition, integrating large-scale PV power generation into the grid presents difficulties owing to its inherent randomness and volatility. This can increase the pressure on the frequency regulation of the grid, posing challenges for the stable operation of new power systems. To address the frequency regulation issues caused by large-scale PV integration, it is essential for PV power stations to possess certain frequency regulation capabilities. These capabilities can help compensate for the capacity reduction associated with replacing conventional thermal power units. In this context, [14] investigated the mandatory frequency-sensitive mode of PV enhanced with high-sensitivity inertial response and its impact on frequency quality. Reference [15] discusses the implications of large-scale PV generation on the frequency stability of power systems. Additionally, the study examines the positive effects of deloaded PV in supporting system frequency recovery during the initial few seconds after major contingencies. In [16], a novel control strategy was developed for frequency regulation using the output from the PV generators without using any storage technologies. The BESS, known for its rapid response to load variations and high precision regulation, is a high-quality resource for frequency regulation. The joint participation of PV generation and BESSs in system frequency regulation offers synergistic benefits. These include improving the accuracy of PV power output and alleviating the frequency regulation pressure on the grid. Reference [17] proposed a framework that uses shared BESSs to fulfill the primary frequency response obligations of multiple wind and PV power stations while simultaneously providing commercial automatic generation control (AGC) services in the ancillary services market. Considering the high costs associated with the cycle life of BESSs, [18] advocated for prioritizing the allocation of grid frequency regulation signals to new energy stations, with the BESSs serving as a supplementary regulation resource. This method effectively avoids frequent actions that could impact the cycle life of BESSs. The comparison of the methods proposed in the above references is shown in Table I.

TABLE I
COMPARISON OF METHODS PROPOSED IN LITERATURE

Reference	Power market			Bidding	Carbon trading	Storage cycle life	AGC	Uncertainty
	Energy market	Frequency regulation market	Real-time balancing market					
[5]	√	√	–	√	–	–	–	√
[6]	√	–	–	√	–	–	√	–
[7]	√	–	√	–	–	–	–	√
[8]	–	–	√	–	–	–	–	–
[9], [10]	√	–	–	–	–	√	–	–
[11]	–	–	√	√	–	–	√	√
[12]	√	–	–	√	√	–	–	–
[13]	–	–	√	–	√	√	√	√
[14]	√	√	–	–	–	–	√	√
[15]	–	√	–	–	–	–	√	√
[16]	–	√	–	–	–	–	√	√
[17]	–	√	√	–	–	√	√	–
[18]	√	√	–	–	–	√	√	√
This paper	√	√	√	√	√	√	√	√

Note: √ represents the item is considered; and – represents the item is not considered.

With energy conservation and emission reduction in PV and BESSs as a focal point, this study aims to improve the economic efficiency of such systems. It proposes a bidding strategy for PV and BESSs operating jointly in energy and frequency regulation markets, with a focus on carbon reduction benefits. The main contributions of this study are as follows.

1) We introduce a two-stage bidding framework that considers real-time energy deviation and various sources of uncertainty. This enables optimized decision-making for the participation of PV and BESSs in the energy market, frequency regulation market, and carbon market over an extended time scale.

2) We suggest a frequency regulation control method applicable across different control intervals. It leverages the strengths of frequency regulation in PV and BESSs, demonstrating excellent performance in situations of urgent frequency fluctuations while considering the operational economics of PV and BESSs.

3) By quantifying carbon emission reduction benefits as

an economic indicator and incorporating the indicator into the objective function, we devise an optimal bidding strategy for PV and BESSs. This strategy can yield considerable carbon emission reduction benefits.

The remainder of this paper is organized as follows. Section II establishes a two-stage bidding framework, focusing on market bidding for PV and BESSs. In Section III, we introduce a real-time frequency regulation control method for PV and BESSs based on partitioning of area control error (ACE) control zones. Section IV describes the bidding strategy optimization. A case study is presented in Section V. Finally, conclusions are presented in Section VI.

II. Two-stage Bidding Framework

Currently, most energy markets globally operate in two stages: the day-ahead energy market and the real-time balancing market. These are jointly cleared in the energy and frequency regulation markets [19], [20]. This study focuses specifically on the carbon trading mechanism in the Chinese market. In China, CCER transactions are categorized into primary and secondary markets based on their functional roles. The primary market is managed by the national regulatory authorities and handles the approval, filing, and issuance of CCER projects. Once new energy companies have registered their emission reduction credits, they are eligible to participate in carbon market trading and fulfillment. The secondary market serves as a spot market for short-term carbon emission reduction trades, where power generation companies can freely buy and sell CCERs according to trading rules.

Our focus lies in the research conducted within the secondary carbon and energy markets on a short-term scale. The carbon market and the day-ahead energy market operate one day in advance, whereas the real-time balancing market operates 15 min before real-time operation. The proposed two-stage bidding framework for the participation of PV and BESSs in market transactions is illustrated in Fig. 1.

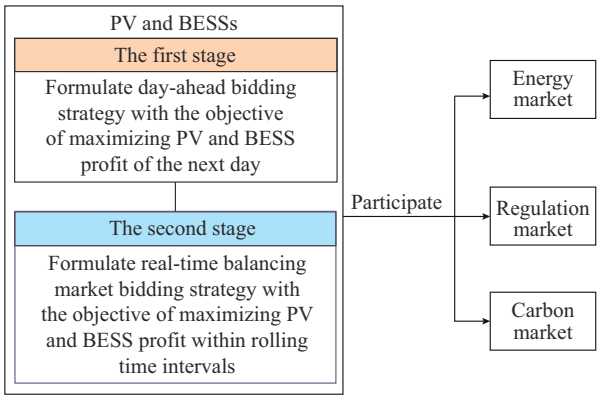

Fig. 1. A Two-stage bidding framework for participation of PV and BESSs in market transactions.

In this framework, it is assumed that the Independent System Operator (ISO) serves as a single buyer, reflecting users' participation in market transactions. Considering the capacity constraints of PV and BESSs, their bidding behavior minimally affects market prices in provincial, regional, or even national unified electricity market and carbon market. Therefore, PV and BESSs are treated as a price taker in electricity market and carbon market, with their declared output accepted by market institutions [21].

In the first stage, which is the bidding optimization stage of the day-ahead energy market, the PV and BESSs submit their bidding output for each time interval of the following day before the closure of the day-ahead energy market. The bidding strategy in this stage is determined based on factors such as the 24-hour PV power forecast data, CCER prices, and predicted electricity prices in both the day-ahead energy market and real-time balancing market. Given the inherent errors in PV power forecasts, particular attention is paid to the potential imbalances between the predicted PV power forecast and actual power. When developing the bidding strategy for the day-ahead energy market, various potential PV power generation scenarios are considered and the expected profits in the real-time balancing market for each scenario are factored into the bidding optimization model of the day-ahead market.

The second stage is the rolling optimization bidding stage in the real-time balancing market. In this stage, the PV and BESSs adjust their day-ahead bidding results according to the latest PV power forecast data and the electricity prices of the real-time balancing market. Every 15 min, the system submits bids for positive and negative balancing of electricity quantities in the real-time balancing market and updates its bidding output for the frequency regulation market. The bidding strategy for the subsequent 4 hours (16 time intervals) is determined using the optimization results from the first time interval within the current rolling window. This iterative process gradually reduces the deviation from the day-ahead bidding plan.

In real-time dispatching, the dispatch center issues AGC commands to the PV and BESSs. This is based on the actual fluctuations of the grid frequency and the frequency regulation capacity reported by the system in the frequency regulation market. The PV and BESSs that are actually called upon receive economic compensation for providing frequency regulation services. The real-time energy quantity and power of the BESSs are adjusted based on the actual PV output data and the frequency regulation capacity undertaken by the PV and BESSs. The updated data serve as an input for the next round of rolling optimization, forming a closed-loop optimization control system. This effectively increases BESS utilization and the benefits of the PV and BESSs.

III. Real-time Frequency Regulation Control Method for PV and BESSs Based on Partitioning of ACE Control Zones

A. Partitioning of ACE Control Zones

In the AGC system, frequency or power deviations in the system prompt the dispatch center to determine the ACE by analyzing and calculating these deviations. The available frequency regulation resources are then assigned according to certain rules. ACE represents the difference between the planned and the actual power outputs within the control area

of the power grid. If ACE is larger than 0, the power output should be proportionately reduced. Conversely, if ACE is smaller than 0, the power output should be correspondingly increased. ACE serves as a pivotal control parameter in the development of real-time frequency regulation control methods for AGC and functions as a key measure of the effectiveness of control methods.

In terms of the actual operation of the power grid, ACE control zones are obtained through the wide-area monitoring system and energy management information system. Typically, the ACE control zones are classified based on the absolute value of ACE and predetermined static threshold values [22]. These zones can be classified into four intervals: the dead zone, emergency regulation zone, sub-emergency regulation zone, and normal regulation zone, as shown in Fig. 2, where A_{CED}, A_{CEA}, and A_{CEE} are the boundary values of the above intervals.

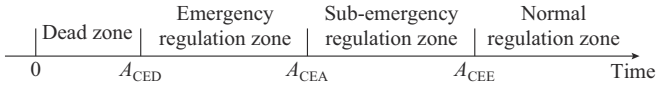

Fig. 2. Partitioning of ACE control zones.

B. Real-time Frequency Regulation Control Method for PV and BESSs Participating in AGC

Compared with traditional frequency regulation resources, BESSs offer a distinct advantage: there are no constraints on ramp rate control. This allows them to rapidly respond to emergency frequency regulation demands within the region. This rapid response capability facilitates the participation of PV and BESSs in grid frequency regulation, effectively addressing the stability issues associated with standalone PV participating in frequency regulation and improving economic viability. To fully harness the frequency response advantages of PV and BESSs, it is necessary to devise appropriate charging and discharging strategies based on the ACE control zone. Additionally, it is important to allocate frequency regulation signals to PV and BESSs according to the corresponding distribution principles.

Different ACE control zones present different levels of urgency for frequency regulation demands at the scheduling center, leading to different control objectives. Based on this, this study proposes a real-time frequency regulation control method that integrates PV and BESSs with AGC. Owing to the faster response than conventional generating units, it is hypothesized that the PV and BESSs should be the first to respond to regional frequency regulation requirements. Any residual frequency regulation capacity that the PV and BESSs are unable to meet is then proportionally distributed to other conventional generating units based on their ramp rates. The specific allocation strategy is outlined as follows.

1) When the ACE is within the emergency control zone, the primary control objective is ensuring grid frequency safety. The goal is to rapidly reduce regional control deviation to the maximum extent, thereby restoring the power system to a stable and safe state. In this phase, the dispatch center mandates the BESSs to perform frequency regulation at its maximum charging/discharging power. Furthermore, there are no limits on the state of charge (SOC) of the BESS during this period. Additionally, the dispatch center will allocate any surplus capacity from the PV power station, beyond its assigned power in the energy market, to frequency regulation. At this time, the regulation capacity $\Delta P^{(1)}_{\mathrm{ACE},t}$ allocated by the AGC system to the PV and BESSs is expressed as:

$$\Delta P^{(1)}_{\mathrm{ACE},t}=\begin{cases}P^{\max}_{\mathrm{c}}-P^{\mathrm{bat}}_{t}-\gamma_1\left(P^{\mathrm{PV_{real}}}_{t}-P^{\mathrm{PVe}}_{t}\right) & ACE>0\\ -P^{\max}_{\mathrm{d}}-P^{\mathrm{bat}}_{t}-\gamma_2\left(P^{\mathrm{PV_{real}}}_{t}-P^{\mathrm{PVe}}_{t}\right) & ACE<0\end{cases} \tag{1}$$

$$\begin{cases}\gamma_1=1,\ \gamma_2=0 & P^{\mathrm{PV_{real}}}_{t}-P^{\mathrm{PVe}}_{t}<0\\ \gamma_1=0,\ \gamma_2=1 & P^{\mathrm{PV_{real}}}_{t}-P^{\mathrm{PVe}}_{t}>0\end{cases} \tag{2}$$

where P^{PVe}_{t} is the winning power of the PV power station in the energy market during period t; $P^{\max}_{\mathrm{c}}$ and $P^{\max}_{\mathrm{d}}$ are the maximum limits for charging and discharging BESSs, respectively; P^{bat}_{t} is the operating power of BESSs during period t; $P^{\mathrm{PV_{real}}}_{t}$ is the actual output value of PV power station during period t; and γ_1 and γ_2 are the regulation coefficients that constrain the priority of the participation of BESSs in grid frequency regulation over tracking the planned PV output. When the maximum available capacity of frequency regulation resources in the region is insufficient to balance grid frequency fluctuations during this period, measures such as emergency load shedding should be implemented to ensure grid safety and stability.

2) When the ACE is within the sub-emergency regulation zone, the BESS operates at full power. In this scenario, the BESS prioritizes tracking the PV output and adjusts its charging and discharging actions to minimize the deviation between the actual and planned PV output. This adjustment considers the constraints imposed by the SOC of BESSs on the maximum charging/discharging power. Simultaneously, the dispatch center uses the surplus capacity of the PV power station in the energy market, beyond the contracted power, for frequency regulation. In this context, the regulation capacity $\Delta P^{(2)}_{\mathrm{ACE},t}$ allocated by the AGC system to the PV and BESSs is expressed as:

$$\Delta P^{(2)}_{\mathrm{ACE},t}=\begin{cases}P^{\max}_{\mathrm{c}}-P^{\mathrm{bat}}_{t}-\left(P^{\mathrm{PV_{real}}}_{t}-P^{\mathrm{PV}}_{t}\right) & ACE>0\\ -P^{\max}_{\mathrm{d}}-P^{\mathrm{bat}}_{t}-\left(P^{\mathrm{PV_{real}}}_{t}-P^{\mathrm{PV}}_{t}\right) & ACE<0\end{cases} \tag{3}$$

where P^{PV}_{t} is the predictive output of PV power stations.

3) When the ACE is within the normal regulation zone, the system remains within the normal operating range, but the ACE reaches the set response threshold ACE_{D}. At this point, the revenue of the PV and BESSs becomes the control objective. Moreover, the dispatch center allocates power according to the upward and downward outputs declared for the PV and BESSs in the real-time balancing market. The extent $\Delta P^{(3)}_{\mathrm{ACE},t}$ of regulation undertaken by the PV and BESSs is expressed as:

$$\Delta P^{(3)}_{\mathrm{ACE},t}=\begin{cases}P^{\mathrm{PV_{dn},RT}}_{t}+P^{\mathrm{C_{dn},RT}}_{t} & ACE>P^{\mathrm{PV_{dn},RT}}_{t}+P^{\mathrm{C_{dn},RT}}_{t}\\ -P^{\mathrm{PV_{up},RT}}_{t}-P^{\mathrm{C_{up},RT}}_{t} & ACE<-P^{\mathrm{PV_{up},RT}}_{t}-P^{\mathrm{C_{up},RT}}_{t}\\ ACE & \text{others}\end{cases} \tag{4}$$

where $P^{\mathrm{PV_{up},RT}}_{t}$ and $P^{\mathrm{PV_{dn},RT}}_{t}$ are the bids for upward and downward outputs from the PV power stations in the regulation market during period t, respectively; and $P^{\mathrm{C_{up},RT}}_{t}$ and $P^{\mathrm{C_{dn},RT}}_{t}$

are the up-regulated and down-regulated outputs from the BESSs in the regulation market during period t, respectively.

4) When the ACE remains within the dead zone, the demand for frequency regulation power in the region is minimal. Under these circumstances, conventional frequency regulation units are sufficient to meet the regional regulation needs. To protect battery life longevity from frequent charging and discharging cycles and to maintain system frequency deviation to a minimum value, the PV and BESSs abstain from participating in grid regulation during this period. Instead, reliance is placed solely on conventional frequency regulation units for maintaining balance. Consequently, the regulation capacity $\Delta P_{\mathrm{ACE},t}^{(4)}$ delegated by the AGC system to the PV and BESSs is expressed as:

$$\Delta P_{\mathrm{ACE},t}^{(4)} = 0 \tag{5}$$

IV. Bidding Strategy Optimization

A. Bidding Model of Day-ahead Energy Market

The bidding model of the day-ahead energy market formulates the strategies that aim to maximize the expected profit of PV and BESSs in different scenarios. The objective function comprises five components: energy market revenue $W^{\mathrm{e,DA}}$, frequency regulation market revenue $W^{\mathrm{r,DA}}$, expected revenue from the real-time balancing market $W^{\mathrm{p,DA}}$, CCER revenues available to PV and BESSs in the carbon market W^{CCER}, and BESS life depreciation cost W^{c}. The objective function is expressed as:

$$\max W^{\mathrm{DA}} = W^{\mathrm{e,DA}} + W^{\mathrm{r,DA}} + W^{\mathrm{p,DA}} + W^{\mathrm{CCER}} - W^{\mathrm{c}} \tag{6}$$

$W^{\mathrm{e,DA}}$ is calculated as:

$$W^{\mathrm{e,DA}} = \sum_{t=1}^{N_t} c_t^{\mathrm{e,DA}} (P_t^{\mathrm{PVe,DA}} + P_t^{\mathrm{dis,DA}} - P_t^{\mathrm{ch,DA}}) \Delta t \tag{7}$$

where N_t is the total number of periods; $c_t^{\mathrm{e,DA}}$ is the electricity price of the day-ahead energy market during period t; $P_t^{\mathrm{PVe,DA}}$ is the bidding output during period t submitted by the PV power station when participating in the bidding of the day-ahead energy market; and $P_t^{\mathrm{dis,DA}}$ and $P_t^{\mathrm{ch,DA}}$ are the discharging and charging power of BESSs in the day-ahead energy market, respectively.

$W^{\mathrm{r,DA}}$ is calculated as:

$$\begin{aligned} W^{\mathrm{r,DA}} = &\sum_{t=1}^{N_t} c_t^{\mathrm{up,DA}} (P_t^{\mathrm{PV_{up},DA}} + P_t^{\mathrm{C_{up},DA}}) \Delta t + \\ &\sum_{t=1}^{N_t} c_t^{\mathrm{dn,DA}} (P_t^{\mathrm{PV_{dn},DA}} + P_t^{\mathrm{C_{dn},DA}}) \Delta t \end{aligned} \tag{8}$$

where $c_t^{\mathrm{up,DA}}$ and $c_t^{\mathrm{dn,DA}}$ are the upward and downward frequency regulation prices during period t, respectively; $P_t^{\mathrm{PV_{up},DA}}$ and $P_t^{\mathrm{PV_{dn},DA}}$ are the declared upward and downward outputs of PV power stations in the frequency regulation markets during period t, respectively; and $P_t^{\mathrm{C_{up},DA}}$ and $P_t^{\mathrm{C_{dn},DA}}$ are the upward and downward outputs of BESSs declared in frequency regulation markets during period t, respectively.

In the day-ahead stage, this study takes into account the possible actual PV output scenarios that may occur in the future and the regulatory role of BESSs within these scenarios. It uses (9) to calculate the expected revenue from the real-time balancing market.

$$W^{\mathrm{p,DA}} = \sum_{s=1}^{N_S} \pi_s \left[\sum_{t=1}^{N_t} (c_t^{\mathrm{up}} \Delta P_{s,t}^{\mathrm{up}} - c_t^{\mathrm{down}} \Delta P_{s,t}^{\mathrm{down}}) \Delta t \right] \tag{9}$$

$$\begin{cases} c_t^{\mathrm{up}} = \min(c_t^{\mathrm{e,DA}}, c_t^{\mathrm{e,RT}}) \\ c_t^{\mathrm{down}} = \max(c_t^{\mathrm{e,DA}}, c_t^{\mathrm{e,RT}}) \end{cases} \tag{10}$$

where N_S is the number of scenarios; π_s is the probability of occurrence for scenario s; c_t^{up} and c_t^{down} are the settlement electricity prices for positive and negative imbalances in the real-time balancing market during period t, respectively; $c_t^{\mathrm{e,RT}}$ is the electricity price of the real-time energy market during period t; and $\Delta P_{s,t}^{\mathrm{up}}$ and $\Delta P_{s,t}^{\mathrm{down}}$ are the positive and negative unbalanced power in scenario s during period t, respectively.

Specifically, the positive unbalanced price is the lower price between the electricity price of the day-ahead energy market and that of real-time balancing market; conversely, the negative unbalanced price is the higher price between the electricity price of the day-ahead energy market and that of the real-time balancing market [23]. The CCER revenues available to PV and BESSs in the carbon market are calculated as:

$$W^{\mathrm{CCER}} = \sum_{s=1}^{N_S} \pi_s \left(\sum_{t=1}^{N_t} K_{\mathrm{c}} c^{\mathrm{CCER}} \phi_{\mathrm{CM}} P_t^{\mathrm{DA}} \Delta t \right) \tag{11}$$

$$\begin{aligned} P_t^{\mathrm{DA}} = &(P_t^{\mathrm{PVe,DA}} + P_t^{\mathrm{dis,DA}} - P_t^{\mathrm{ch,DA}}) + \\ &(P_t^{\mathrm{PV_{up},DA}} + P_t^{\mathrm{C_{up},DA}} - P_t^{\mathrm{PV_{dn},DA}} - P_t^{\mathrm{C_{dn},DA}}) + (\Delta P_{s,t}^{\mathrm{up}} - \Delta P_{s,t}^{\mathrm{down}}) \end{aligned} \tag{12}$$

where K_{c} is the indicator that represents the historical performance of PV and BESSs in the CCER market; c^{CCER} is the CCER price; P_t^{DA} is the day-ahead planned power during period t; and ϕ_{CM} is the grid marginal emission factor, which is the carbon emission reduction generated by the PV and BESSs for every 1 MWh of electricity generated. This study takes the average level of marginal emission factors of the Chinese power grid as 0.7568 tCO_2/MWh.

Considering the frequent frequency regulation instructions from the power grid, which are difficult to accurately predict, the BESSs need to respond to each frequency regulation signal in every control cycle. This is achieved through charging and discharging under the actual frequency regulation conditions. Therefore, the model of the BESS life depreciation cost requires appropriate adjustment.

$$\begin{aligned} W^{\mathrm{c}} = &\sum_{s=1}^{N_S} \pi_s \sum_{t=1}^{N_t} c^{\mathrm{o}} (P_t^{\mathrm{dis,DA}} + P_t^{\mathrm{ch,DA}}) \Delta t + \\ &\sum_{s=1}^{N_S} \pi_s \sum_{t=1}^{N_t} c^{\mathrm{o}} \left[2\varepsilon (P_t^{\mathrm{C_{up},DA}} + P_t^{\mathrm{C_{dn},DA}}) + \left| P_{s,t}^{\mathrm{PVbat}} \right| \right] \Delta t \end{aligned} \tag{13}$$

where $P_{s,t}^{\mathrm{PVbat}}$ is the charging/discharging power of BESSs tracking the PV output plan during period t; c^{o} is the cost coefficient for BESS life loss; ε is the frequency regulation power coefficient, which indicates that the BESSs will charge or discharge ε MWh of energy to provide 1 MW of frequency regulation power in actual operation [24], [25]. Given that the average value of the frequency regulation signal during a control cycle is approximately 0, 2ε is used to represent the average value of the total charging/discharging amount of BESSs. The value of ε is generally taken as 0.24.

The constraints related to the participation of the PV and BESSs in the bidding process of the day-ahead energy mar-

ket are specified as:

$$P_{s,t}^{\mathrm{PVreal}}=P_t^{\mathrm{PVe,DA}}+P_t^{\mathrm{PV_{up},DA}}-P_t^{\mathrm{PV_{dn},DA}}+\Delta P_{s,t}^{\mathrm{up}}-\Delta P_{s,t}^{\mathrm{down}}+P_{s,t}^{\mathrm{PVbat}} \tag{14}$$

$$P_{s,t}^{\mathrm{bat}}=P_{s,t}^{\mathrm{PVbat}}-P_t^{\mathrm{dis,DA}}+P_t^{\mathrm{ch,DA}}-P_t^{\mathrm{C_{up},DA}}+P_t^{\mathrm{C_{dn},DA}} \tag{15}$$

$$0\le P_t^{\mathrm{PVe,DA}}\le P_t^{\mathrm{PV,DA}} \tag{16}$$

$$0\le P_t^{\mathrm{PV_{up},DA}}\le P_t^{\mathrm{PV,DA}}-P_t^{\mathrm{PVe,DA}} \tag{17}$$

$$0\le P_t^{\mathrm{PV_{dn},DA}}\le P_t^{\mathrm{PVe,DA}} \tag{18}$$

$$0\le \Delta P_{s,t}^{\mathrm{up}}\le u_{s,t}M_1 \tag{19}$$

$$0\le \Delta P_{s,t}^{\mathrm{down}}\le (1-u_{s,t})M_2 \tag{20}$$

$$0\le P_t^{\mathrm{ch,DA}}\le P_{\mathrm{c}}^{\max} \tag{21}$$

$$0\le P_t^{\mathrm{dis,DA}}\le P_{\mathrm{d}}^{\max} \tag{22}$$

$$0\le P_t^{\mathrm{C_{dn},DA}}\le P_{\mathrm{c}}^{\max} \tag{23}$$

$$0\le P_t^{\mathrm{C_{up},DA}}\le P_{\mathrm{d}}^{\max} \tag{24}$$

$$0\le P_t^{\mathrm{ch,DA}}+P_t^{\mathrm{C_{dn},DA}}\le P_{\mathrm{c}}^{\max} \tag{25}$$

$$0\le P_t^{\mathrm{dis,DA}}+P_t^{\mathrm{C_{up},DA}}\le P_{\mathrm{d}}^{\max} \tag{26}$$

$$E_{s,t}=E_{s,t-1}+P_{s,t}^{\mathrm{bat}}\eta_{\mathrm{c}}\Delta t \quad P_{s,t}^{\mathrm{bat}}>0 \tag{27}$$

$$E_{s,t}=E_{s,t-1}+\frac{P_{s,t}^{\mathrm{bat}}\Delta t}{\eta_{\mathrm{d}}} \quad P_{s,t}^{\mathrm{bat}}<0 \tag{28}$$

$$-E_{s,t}+SOC_{\min}\cdot E_{\mathrm{bat}}\le 0 \tag{29}$$

$$E_{s,t}-SOC_{\max}\cdot E_{\mathrm{bat}}\le 0 \tag{30}$$

where $P_{s,t}^{\mathrm{bat}}$ is the operating power of BESSs in scenario s during period t, and $P_{s,t}^{\mathrm{bat}}>0$ and $P_{s,t}^{\mathrm{bat}}<0$ mean that the BESSs are charging and discharging, respectively; $u_{s,t}$ is the binary variable characterizing the unbalanced power state; $P_t^{\mathrm{PV,DA}}$ is the predictive output of PV power stations during period t; $SOC_{\min}$ and $SOC_{\max}$ are the minimum and maximum values of the SOC for BESSs, respectively; $E_{s,t}$ is the remaining power of BESSs in scenario s during period t; E_{bat} is the rated capacity of BESSs; η_{c} and η_{d} are the charging and discharging efficiencies of BESSs, respectively; and M_1 and M_2 are the notably large positive numbers.

Constraint (14) indicates that the bidding power of the PV and BESSs should be limited by the actual output of the system. Constraint (15) indicates that the operational power of BESSs during period t is related to the bidding power of BESSs and the charging/discharging power coordinated with the PV system. Constraints (16)-(18) denote the constraints specific to PV stations. Constraint (16) states that the bidding power of PV stations should not exceed the forecasted output of the PV and this bidding power should be non-negative. Constraint (17) represents the upward regulation power of PV generation participating in the frequency regulation market, considering the difference between the forecasted output of PV stations and their bidding power in the energy market. Constraint (18) describes the downward regulation power of PV stations in the frequency regulation market, factoring in the effect of the bidding power in the energy market. Similar to the upward regulation power, the downward regulation power of PV station in the frequency regulation market should also be non-negative. Constraints (19) and (20) use binary variables to define system imbalances and describe positive and negative unbalanced power. By incorporating objective functions (9) and (12) along with constraints (19) and (20), the coupling relationship between the day-ahead energy market and real-time balancing market is considered in the bidding strategy of the PV and BESSs. Constraints (21)-(26) represent the power constraints for the participation of BESSs in the market. During the charging and discharging processes, the power of the BESS should not exceed its maximum allowable limit. Constraints (27) and (28) relate the remaining energy level of BESSs during any given period to the remaining energy level of the preceding period and charging/discharging power of the current period. The SOC of the BESS is calculated as the ratio of its remaining energy to its rated energy capacity. To prevent any detrimental impacts on the battery lifespan caused by overcharging or excessive discharging, certain range constraints such as (29) and (30) are imposed on the SOC of the BESS to ensure its operation within safe levels.

B. Bidding Model of Real-time Balancing Market

PV stations often face considerable forcast errors with respect to electricity prices and output power. Therefore, the PV and BESSs bid for positive and negative imbalanced power in the real-time balancing market to maintain their own energy balance. This study adopts a rolling optimization method and establishes a bidding optimization model of the real-time balancing market based on the latest PV output forecasts and real-time balancing market prices. The objective of the model is to maximize the profit of the PV and BESSs during the rolling period within the real-time balancing market. The objective function is represented by (31). The constraints applicable in the real-time balancing market are generally similar to those in the day-ahead energy market, eliminating the need for redundant explanation.

$$\max W^{\mathrm{RT}}=W^{\mathrm{p,RT}}+W^{\mathrm{r,RT}}-W^{\mathrm{pen}}-W^{\mathrm{c}} \tag{31}$$

where W^{RT} is the objective function of the bidding model of the real-time balancing market; $W^{\mathrm{p,RT}}$ is the revenue of the PV and BESSs from the real-time balancing market; $W^{\mathrm{r,RT}}$ is the revenue of the PV and BESSs from the frequency regulation market; and W^{pen} is the output deviation penalty cost of the PV and BESSs.

W^{pen} is calculated as:

$$W^{\mathrm{pen}}=\sum_{t=1}^{N_t}\alpha c_t^{\mathrm{e,RT}}(P_t^{\mathrm{DA}}-P_t^{\mathrm{RT}})\Delta t \quad P_t^{\mathrm{DA}}<P_t^{\mathrm{RT}} \tag{32}$$

$$\begin{aligned}P_t^{\mathrm{RT}}=&(P_t^{\mathrm{PVe,DA}}+P_t^{\mathrm{dis,DA}}-P_t^{\mathrm{ch,DA}})+\\&(P_t^{\mathrm{PV_{up},RT}}+P_t^{\mathrm{C_{up},RT}}-P_t^{\mathrm{PV_{dn},RT}}-P_t^{\mathrm{C_{dn},RT}})+(\Delta P_t^{\mathrm{up,RT}}-\Delta P_t^{\mathrm{down,RT}})\end{aligned} \tag{33}$$

where α is the deviation penalty coefficient; P_t^{RT} is the real-time planning of online power for PV and BESSs; and $\Delta P_t^{\mathrm{up,RT}}$ and $\Delta P_t^{\mathrm{down,RT}}$ are the positive and negative unbalanced power of the PV and BESS bidding during period t, respectively.

Once the PV and BESSs report the bidding power for the current period, the dispatch center responds by issuing AGC

instructions, which are formulated based on the actual fluctuations in grid frequency and the frequency regulation capacity that the PV and BESSs report in the frequency regulation market. Considering the uncertainty of the actual PV output, along with the impact of real-time AGC instructions on the power and energy levels of BESSs, it becomes necessary to make adjustments at the end of each rolling window. This is a crucial step as these factors can influence the initial state of BESSs when they participate in the market subsequently.

$$P_t^{\text{batoper}} = P_t^{\text{PVreal}} - (P_t^{\text{PVe,DA}} + P_t^{\text{dis,DA}} - P_t^{\text{ch,DA}}) - (\Delta P_t^{\text{up}} - \Delta P_t^{\text{down}}) + \Delta P_{\text{ACE},t} \tag{34}$$

$$P_t^{\text{batoper}\prime} = \begin{cases} P_{\text{c}}^{\max} & P_t^{\text{batoper}} > P_{\text{c}}^{\max} \\ P_t^{\text{batoper}} & -P_{\text{d}}^{\max} \le P_t^{\text{batoper}} \le P_{\text{c}}^{\max} \\ -P_{\text{d}}^{\max} & P_t^{\text{batoper}} < -P_{\text{d}}^{\max} \end{cases} \tag{35}$$

where P_t^{batoper} is the corrected BESS operating power; $P_t^{\text{batoper}\prime}$ is the BESS operating power adjusted again after the first correction when the BESS operating power exceeds the limit; ΔP_t^{up} and ΔP_t^{down} are the positive and negative unbalanced power during period t, respectively; and $\Delta P_{\text{ACE},t}$ is the actual frequency regulation of PV and BESSs.

Based on (34) and (35), the actual frequency regulation amount of the PV and BESSs is obtained using the real-time frequency regulation control method proposed in Section III. Furthermore, it becomes necessary to recalculate the BESS capacity based on (27) and (28). These real-time operational output variables serve as input variables for the next time step, thus continuing the rolling optimization process to develop the optimal bidding strategy. In summary, the trading method in the energy and frequency regulation markets is shown in Fig. 3.

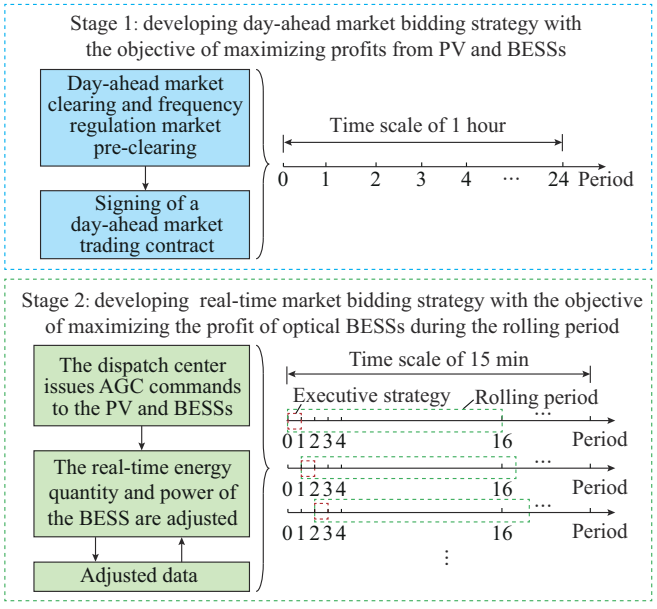

Fig. 3. Trading method in energy and frequency regulation markets.

V. Case Study

A. Simulation Settings

To verify the feasibility and superiority of the proposed bidding strategy, we conducted a case study using a 40 MW PV station as an example. Its associated BESSs have a rated capacity and maximum charging/discharging power of 10 MWh and 5 MW, respectively. The remaining parameters of the integrated system are set according to Table II. The simulations are performed using MATLAB R2016b, invoking the established commercial solver Cplex.

TABLE II
System Parameter Settings

c^{o} (¥/MW)	η_{c}	η_{d}	$SOC_{\min}$	$SOC_{\max}$	α
20	0.9	0.9	0.15	0.9	0.1

The PV and BESSs participate in market transactions as a receiver of market prices, submitting bids without specifying prices. The day-ahead energy and real-time balancing markets settle based on their respective nodal marginal prices. In this study, we used the historical trial operation data regarding prices of the energy market and frequency regulation market from Jiangsu, China [26]. These data are used to generate forecasted electricity prices for the day-ahead energy market and real-time balancing market, as shown in Fig. 4, where the time interval between periods is 15 min.

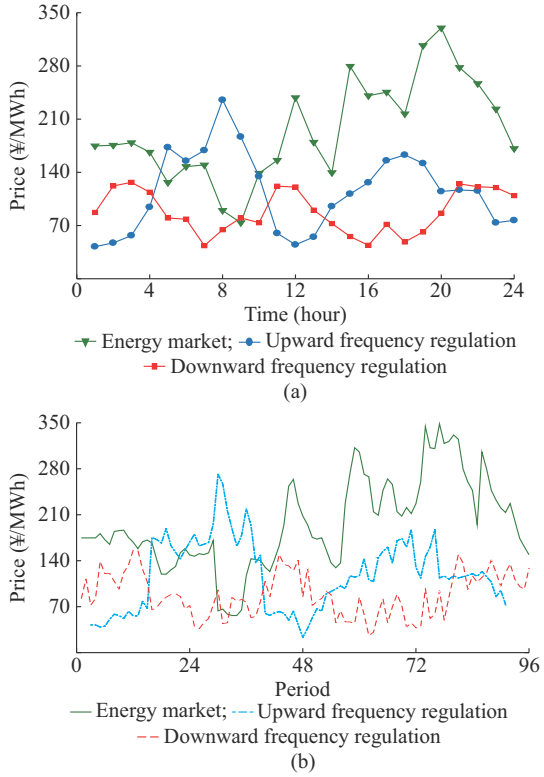

Fig. 4. Forecasted electricity prices in day-ahead energy market and real-time balancing market. (a) Day-ahead energy market. (b) Real-time balancing market.

B. Set of PV Output Uncertainty Scenarios

The historical generation data selected for analysis in this study spans from June to July 2018 and originates from a 40 MW PV station. A time-series modeling approach, based on an hourly clear-sky index [27], is employed to forecast the

day-ahead and real-time PV outputs. The predicted output curves of the PV station are illustrated in Fig. 5.

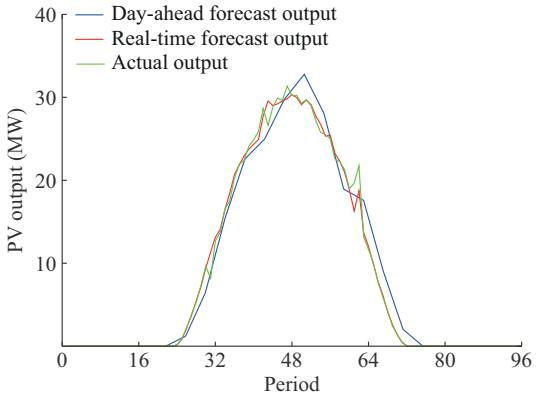

Fig. 5. Predicted output curves of PV station.

Considering the uncertainties caused by factors such as environmental temperature and weather conditions, the predicted PV output is not immune to errors. Moreover, these prediction errors exhibit a pattern wherein predictions closer in time are more accurate than those further away. This is based on the time scale of the predictions. In this study, particular attention is paid to the probability modeling analysis of the day-ahead PV output prediction errors. Compared with day-ahead predictions, real-time predictions demonstrate higher accuracy and align more closely with the operational timeframe of the real-time balancing market. Therefore, extensive simulations using the scenario approach to analyze real-time PV prediction errors are no longer necessary, thus enhancing operational efficiency.

Assuming that the prediction errors of PV output for each time interval in the day-ahead market follow a normal distribution with a standard deviation set at 5% of the predicted value, a Monte Carlo sampling method is employed to randomly generate 100 scenarios of PV output, as shown in Fig. 6(a).

To reduce computational time and complexity, the *K*-means clustering algorithm is used to reduce the number of scenarios. The number of clustered scenarios is set to be 4, resulting in typical PV output scenarios (Scenarios 1-4), as depicted in Fig. 6(b). The probabilities of Scenarios 1-4 are 0.26, 0.36, 0.14, and 0.24, respectively. The reduced set of scenarios closely resembles the original set, effectively capturing variations in PV output trends. Additionally, the reduced number of scenarios reduces the complexity of subsequent optimization studies and computational requirements.

C. Impact of PV and BESSs Participating in Market Behavior on Revenues

In this subsection, two different conditions are presented to assess how the participation of the PV and BESSs in the energy and frequency regulation markets affects revenues.

1) Condition 1: the PV and BESSs participate in the energy and frequency regulation markets simultaneously.

2) Condition 2: the PV and BESSs exclusively participate in the energy market.

Figure 7 depicts the results of optimal bidding strategy under Condition 1.

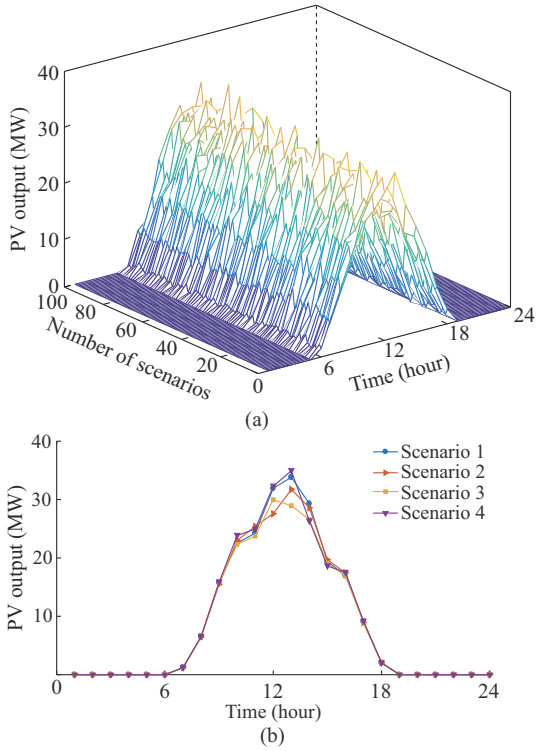

Fig. 6. Scenarios of PV output and typical PV output scenarios. (a) Scenarios of PV output. (b) Typical PV output scenarios.

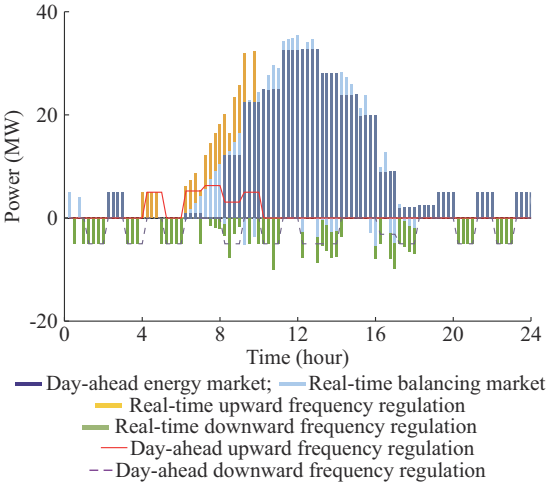

Fig. 7. Results of optimal bidding strategy under Condition 1.

From Fig. 7, it is evident that during the 5th-10th hours, wherein upward frequency regulation prices are higher, the PV and BESSs tend to reserve a portion of frequency regulation capacity for upward frequency regulation services. Conversely, after the 10th hour, when energy market prices are higher, the PV and BESSs provide higher power output bids to participate in the energy market. This strategic bidding approach is employed by the PV and BESSs to maximize the benefits. Additionally, the incorporation of BESSs allows the system to maintain output during the periods of no sunlight or cloudy conditions (insufficient solar radiation). It also enables adjustment of the PV output to align with the periods that generate higher profits based on market prices. As a re-

sult, the economics and flexibility of the PV and BESSs exhibit a substantial enhancement.

Figure 8 illustrates the results of optimal bidding strategy under Condition 2. Table III presents the revenue and cost results of the PV and BESSs under these two conditions. The results reveal that the net profit increases by 15.79% under Condition 1 compared with that under Condition 2. Under Condition 2, no revenue will be generated from the frequency regulation market. However, under Condition 1, economic benefits can be obtained from both energy and frequency regulation markets. This is due to the fact that system operators purchase auxiliary services at higher prices to regulate system frequency. Despite the increased uncertainty and higher penalty costs associated with the frequency regulation market, as well as the increased degradation costs owing to frequent charging and discharging cycles, the overall net profit significantly improves. Although additional uncertainties and costs are involved, the overall gain in net profit is substantial.

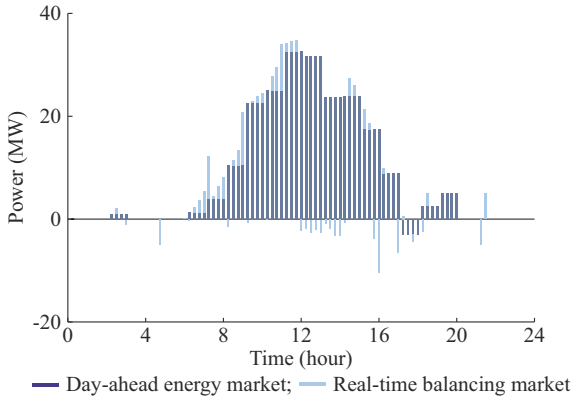

Fig. 8. Results of optimal bidding strategy under Condition 2.

TABLE III
REVENUE AND COST RESULTS OF PV AND BESSS IN DIFFERENT MARKETS

Condition	Revenue (¥)				Penalty cost (¥)	Depreciation cost of BESS life (¥)	Net profit (¥)
	Day-ahead energy market	Carbon market	Real-time balancing market	Frequency regulation market			
1	45269	2684	4897	1982	432	2620	51780
2	40135	2684	1077	0	314	961	42621

Figure 9 illustrates the net profits of the PV and BESSs under two conditions during different periods.

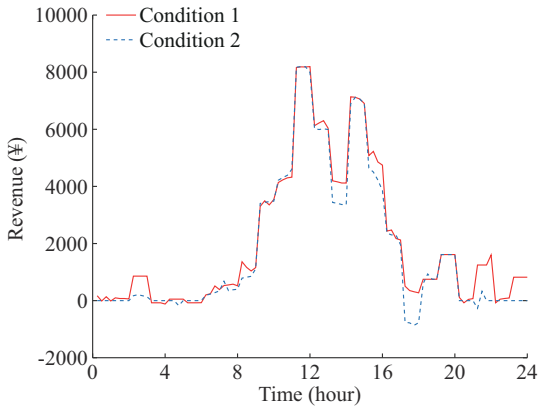

Fig. 9. Comparison of net profits PV and BESSs under two conditions during different periods.

Under Condition 2, the profits are significantly affected by a substantial decrease in the prices of the energy market, evident in the 14th hour. In the 17th hour, the real-time forecasted output of the PV station falls short of the previous forecasted output, requiring the PV and BESSs to purchase negative imbalanced power in the real-time balancing market to maintain the energy balance. Consequently, this results in a dip into negative profit for that period. A higher net profit is generally recorded during each period under Condition 1 compared with that under Condition 2. This can be attributed to two main factors. First, the prices in the frequency regulation market are typically higher than those in the energy market during certain periods. Second, the PV and BESSs reduce the expenses in the real-time balancing market by providing downward frequency regulation services, thereby boosting its overall profits.

D. Analysis of Different BESS Capacities

To show the impact of different BESS capacities on the revenue performance under the two conditions, the revenue and cost results of PV and BESSs participating in different markets with different BESS capacities are shown in Table IV. As shown in Table IV, the increase in storage capacity, which means that the BESSs can store more energy for a longer period, can improve the competitiveness of the PV and BESSs in markets. The larger BESS capability enables the BESSs to better adapt to the demands of the energy and frequency regulation markets and optimize the release and storage of energy based on market prices, thereby increasing the revenue of BESSs in the day-ahead energy market and frequency regulation market.

E. Analysis of Different PV Outputs

To show the impact of different PV outputs on the revenue performance under the two conditions, the revenue results of PV and BESSs participating in different markets under different seasons are shown in Table V. The selected historical data of summer encompass the timeframe of June to July 2018 from a 40 MW PV station, while the historical data of winter encompass the timeframe of November to December 2018.

As shown in Table V, although the light intensity and random fluctuations in winter and summer are different, which leads to a decrease in the revenue of BESSs, the proposed method can still enable PV to benefit under Condition 1, demonstrating the practicality of the proposed method.

TABLE IV
REVENUE AND COST RESULTS OF PV AND BESSS IN DIFFERENT MARKETS WITH DIFFERENT BESS CAPACITIES

Condition	Capacity (MWh)	Revenue (¥)				Penalty cost (¥)	Depreciation cost of BESS life (¥)	Net profit (¥)
		Day-ahead energy market	Carbon market	Real-time balancing market	Regulation market			
1	5	39205	2674	1077	0	319	485	42152
	10	40135	2684	1077	0	314	961	42621
	15	40733	2694	1077	0	306	855	43343
2	5	43013	2667	4751	1786	443	2307	49467
	10	45269	2684	4897	1982	432	2620	51780
	15	46275	2698	5214	2429	424	2905	53287

TABLE V
REVENUE AND COST RESULTS OF PV AND BESSS IN DIFFERENT MARKETS WITH DIFFERENT PV OUTPUTS

Condition	Season	Revenue (¥)				Penalty cost (¥)	Depreciation cost of BESS life (¥)	Net profit (¥)
		Day-ahead energy market	Carbon market	Real-time balancing market	Frequency regulation market			
1	Summer	45269	2684	4897	1982	432	2620	51780
	Winter	29333	2189	4478	1785	326	2581	34878
2	Summer	40135	2684	1077	0	314	961	42621
	Winter	24831	2189	849	0	274	924	26671

F. Analysis of Effectiveness of Frequency Control Strategies

In this study, actual AGC data from a specific region in Jiangsu, China is utilized for simulation. Two scenarios are set up for comparative analysis.

1) Scenario 1: the PV and BESSs participate in the energy market simultaneously, considering the frequency regulation allocation based on the AGC zoning control method.

2) Scenario 2: the PV and BESSs participate in the energy market without considering AGC frequency regulation signals.

Figure 10 presents a comparative assessment of the frequency regulation performance of the PV and BESSs in both scenarios. During period A, the ACE in the region is negligible. In Scenario 1, considering the adverse impact of frequent charging and discharging cycles on the lifespan of BESSs, the decision is made for the PV and BESSs to abstain from participating in the system frequency regulation at this moment, resulting in a regulation allocation of 0 MW. However, in Scenario 2, the BESS adjusts its operations according to the bidding plan to maximize the benefits of the PV and BESSs. At this point, the BESSs adjust upward by 1.03 MW.

During period B, the ACE is within the normal regulation zone. Both Scenarios 1 and 2 are designed with the aim to increase the revenue of the PV and BESSs. At this stage, the system tends to reserve a portion of frequency regulation capacity to participate in the higher-price frequency regulation market. As a result, the PV and BESSs have an allocated regulation capacity of 7.81 MW.

During period C, the ACE surpasses the safe range, indicating an urgent requirement for regulation zone to swiftly return the system to a safe and stable state. However, in Scenario 2, owing to the higher prices in the real-time balancing market at this time (as shown in Fig. 4), the PV and BESSs plan to allocate all excess power above the contracted energy quantity to the real-time balancing market, bypassing system frequency regulation. To rapidly reduce regional frequency deviations, Scenario 1 enforces full power participation of the BESSs in frequency regulation, disregarding the impact of the SOC of the BESS on its maximum charging or discharging power. In addition, the PV generation plan is used for frequency regulation. In this case, the PV and BESSs adjust upward by 7.47 MW.

During period D, the ACE is in the sub-emergency regulation zone. Scenario 1 adopts a zoning control method with the primary objective of ensuring system frequency safety and stability. The BESSs are enforced to participate in frequency regulation at full power, resulting in a regulation allocation of −10 MW provided by the dispatch center. However, in Scenario 2, the PV and BESSs adhere to the day-ahead bidding plan and release 5 MW of energy into the energy market without participating in downward frequency regulation.

A revenue comparison between the two scenarios is shown in Table VI. Given the close correlation between the real-time AGC frequency control process and the real-time balancing market, the revenue from the day-ahead energy market and carbon market remains static. In Scenario 1, the PV and BESSs sacrifice a portion of their revenue in the real-time balancing market to meet the frequency regulation needs of the power grid when the grid control deviation exceeds the safe range. Consequently, this leads to a decrease in revenue from the real-time balancing market. The total daily revenue for the PV and BESSs in Scenario 1 is ¥54832, representing a 3.11% decrease compared with the total revenue in Scenario 2, where the system consistently participates in market bidding to maximize its own interests.

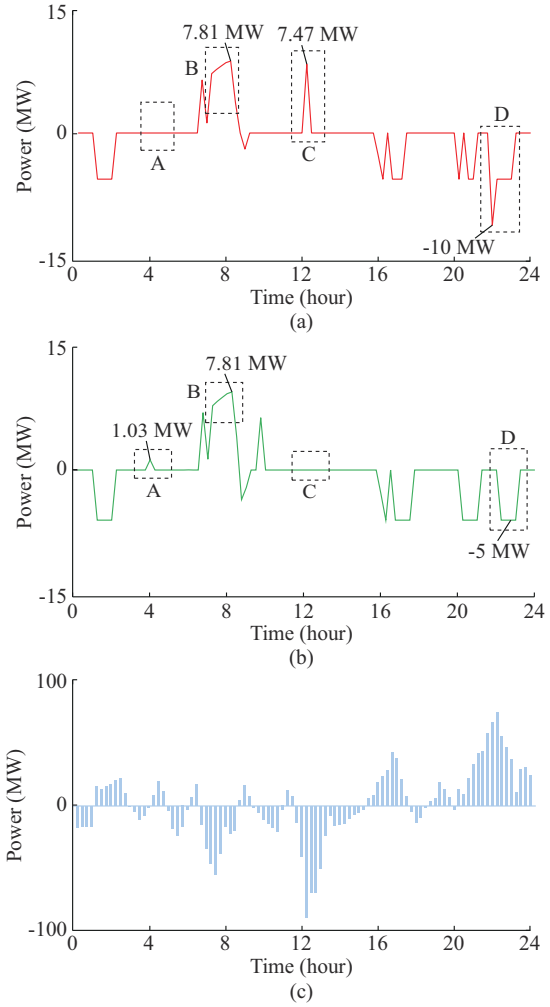

Fig. 10. Frequency regulation performance of PV and BESSs in two scenarios. (a) Scenario 1. (b) Scenario 2. (c) ACE.

TABLE VI
REVENUE COMPARISON BETWEEN TWO SCENARIOS

Scenario	Revenue (¥)				
	Day-ahead energy market	Carbon market	Real-time balancing market	Frequency regulation market	Total
1	45269	2684	1982	4897	54832
2	45269	2684	2857	5726	56536

G. Analysis of Carbon Emission Reduction Benefits

Table VII shows the carbon emission reduction benefits derived from joint bidding for PV and BESSs and separate bidding for PV stations, as determined by the applied model. It is clear that the inclusion of BESSs enhances the grid power output of the PV station by 1.01 MWh during its operation. The number of tons of CCER that new energy power producers can provide is equal to their online electricity consumption multiplied by the marginal emission factor of the power grid. The carbon reduction emissions of PV and BESSs are calculated using the average marginal emission factor in the power grid of China, which is currently at 0.7568 tCO_2/MWh. The data reveal that the PV and BESSs are calculated can reduce carbon emissions by 0.76 t and save an extra 0.32 t of standard coal (assuming that 1 MWh of PV generation replacing standard coal equates to 0.32 t). Considering a CCER price of 20 ¥/t [28], the carbon reduction benefits obtained by BESSs in the carbon market are ¥2684. This represents 6.30% of the total revenue of the operating day, underscoring the considerable additional carbon asset income that CCER introduces to the PV and BESSs.

TABLE VII
ANALYSIS OF CARBON EMISSION REDUCTION BENEFITS

Unit	Grid power (MWh)	Carbon emission (tCO_2)	Solar energy substitution for standard coal consumption (t)	Carbon market revenue (¥)
PV and BESSs	208.63	157.89	66.76	2684
PV station	207.62	157.13	66.44	2515

Upon closer examination of the financial implications of implementing a CCER project with the PV and BESSs, it is found that the certification verification cost of a PV station, with an installed capacity ranging from 10 to 100 MW, typically falls between ¥100000 and ¥300000. It is important to point out that the actual carbon market transactions often experience significant fluctuations in CCER prices. Assuming these fluctuations range between 10 and 40 ¥/t, we can calculate the payback period for the CCER project application of a PV station equipped with a 10 MWh BESS within the aforementioned capacity range. This assessment takes into account only the carbon emission reduction benefits obtained by the PV and BESSs, which is intended to offset the verification costs of the CCER project, as shown in Fig. 11.

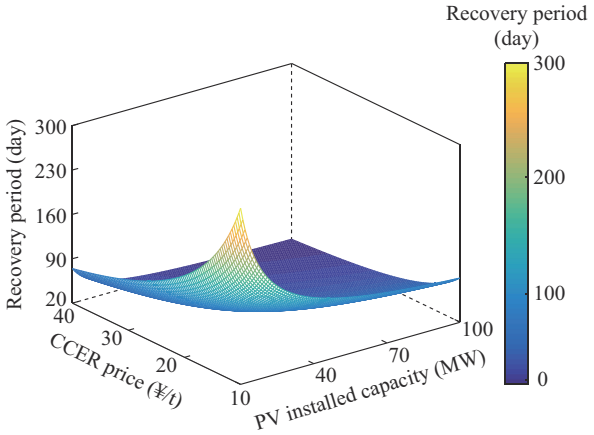

Fig. 11. Recovery status of CCER project.

It can be observed that the carbon emission reduction benefits of the PV and BESSs increase with increasing CCER prices. This enables faster cost recovery and profitability from CCER project verification. Given the same CCER price conditions, the larger-capacity PV and BESSs generate more electricity for the power grid, resulting in higher carbon market income obtained through the CCER mechanism. Therefore, the development of CCER projects yields greater benefits. In recent years, there has been a clear surge in the demand for CCER trading. The carbon emission reduction benefits contribute to the enterprise value of new energy sta-

tions, thereby further enhancing their value. Rational development of CCER projects greatly improves the revenue for large-scale PV stations or regionally distributed PV projects with centralized declarations. This significantly shortens the payback period for investments in PV and BESSs and promotes the sustainable and long-term development of these storage projects.

VI. Conclusion

This study proposes an optimal bidding strategy for PV and BESSs, which is applicable in both energy market and frequency regulation market. This strategy considers carbon reduction benefits and is developed in the context of the new electricity carbon coupling market environment. Case studies based on real-world market prices are conducted to verify the effectiveness of the proposed bidding strategy. The primary findings of the case studies are as follows.

1) The established two-stage bidding framework effectively reduces the impact of uncertainty on the bidding strategy of PV and BESSs. This paves the way for optimal decision-making when participating in the energy, frequency regulation, and carbon markets. In this study, the net profit of the PV and BESSs increases by 21.49% through simultaneous participation in the energy and frequency regulation markets.

2) The proposed real-time frequency regulation control method maintains a good balance between benefit pursuit and frequency regulation fulfillment. It optimally harnesses the potential of the PV and BESSs to provide frequency regulation services, even though a slight 3.11% reduction in profit is observed with the parameters used in our case studies.

3) As demonstrated in the case studies, participation in the carbon market provides a new opportunity for PV and BESSs to earn additional carbon emission reduction benefits, which in turn increases the overall revenue. In this study, the carbon reduction benefits obtained from the PV and BESSs in the carbon market account for 6.30% of the total revenue for the operating day.

In future research, we will consider the shortcomings of user incentive mechanisms and conduct studies on the bidding strategy for PV and BESSs, focusing on their participation in the carbon market and medium-to-long-term energy market.

References

[1] Y. Sun, Y. Zhou, S. Wang *et al*., "Nonparametric probabilistic prediction of regional PV outputs based on granule-based clustering and direct optimization programming," *Journal of Modern Power Systems and Clean Energy*, vol. 11, no. 5, pp. 1450-1461, Sept. 2023.

[2] G. N. D. de Doile, P. Rotella Jr, L. C. S. Rocha *et al*., "Feasibility of hybrid wind and photovoltaic distributed generation and battery energy storage systems under techno-economic regulation," *Renewable Energy*, vol. 195, pp. 1310-1323, Aug. 2022.

[3] T. Liu, P. Wang, Q. Peng *et al*. "Operation-area-constrained adaptive primary frequency support strategy for electric vehicle clusters," *Journal of Modern Power Systems and Clean Energy*, vol. 11, no. 6, pp. 1982-1994, Nov. 2023.

[4] A. A. S. de la Nieta, J. Contreras, and J. I. Munoz, "Optimal coordinated wind-hydro bidding strategies in day-ahead markets," *IEEE Transactions on Power Systems*, vol. 28, no. 2, pp. 798-809, May 2013.

[5] A. Gonzalez-Garrido, A. Saez-de-Ibarra, H. Gaztanaga *et al*., "Annual optimized bidding and operation strategy in energy and secondary reserve markets for solar plants with storage systems," *IEEE Transactions on Power Systems*, vol. 34, no. 6, pp. 5115-5124, Nov. 2019.

[6] L. Argiolas, M. Stecca, L. M. Ramirez-Elizondo *et al*., "Optimal battery energy storage dispatch in energy and frequency regulation markets while peak shaving an EV fast charging station," *IEEE Open Access Journal of Power and Energy*, vol. 9, pp. 374-385, Aug. 2022.

[7] Y. Xie, W. Guo, Q. Wu *et al*., "Robust MPC-based bidding strategy for wind storage systems in real-time energy and regulation markets," *International Journal of Electrical Power & Energy Systems*, vol. 124, p. 106361, Jan. 2021.

[8] A. M. Abomazid, N. A. El-Taweel, and H. E. Z. Farag, "Optimal energy management of hydrogen energy facility using integrated battery energy storage and solar photovoltaic systems," *IEEE Transactions on Sustainable Energy*, vol. 13, no. 3, pp. 1457-1468, Jul. 2022.

[9] Z. Qiu, W. Zhang, S. Lu *et al*., "Charging rate based battery energy storage system model in wind farm and battery storage cooperation bidding problem," *CSEE Journal of Power and Energy Systems*, vol. 8, no. 3, pp. 659-668, May 2022.

[10] M. Aldaadi, F. Al-Ismail, A. T. Al-Awami *et al*., "A coordinated bidding model for wind plant and compressed air energy storage systems in the energy and ancillary service markets using a distributionally robust optimization approach," *IEEE Access*, vol. 9, pp. 148599-148610, Oct. 2021.

[11] A. Saez-de-Ibarra, A. Milo, H. Gaztanaga *et al*., "Co-optimization of storage system sizing and control strategy for intelligent photovoltaic power plants market integration," *IEEE Transactions on Sustainable Energy*, vol. 7, no. 4, pp. 1749-1761, Oct. 2016.

[12] Y. Wen, Y. Chen, P. Wang *et al*., "Photovoltaic-electric vehicles participating in bidding model of power grid that considers carbon emissions," *Energy Reports*, vol. 8, pp. 3847-3855, Nov. 2022.

[13] R. Ma, K. Li, X. Li *et al*., "An economic and low-carbon day-ahead Pareto-optimal scheduling for wind farm integrated power systems with demand response," *Journal of Modern Power Systems and Clean Energy*, vol. 3, no. 3, pp. 393-401, May 2015.

[14] B. I. Craciun, T. Kerekes, D. Sera *et al*., "Frequency support functions in large PV power plants with active power reserves," *IEEE Journal of Emerging and Selected Topics in Power Electronics*, vol. 2, no. 4, pp. 849-858, Dec. 2014.

[15] C. Rahmann and A. Castillo, "Fast frequency response capability of photovoltaic power plants: the necessity of new grid requirements and definitions," *Energies*, vol. 7, no. 10, pp. 6306-6322, Sept. 2014.

[16] P. P. Zarina, S. Mishra, and P. C. Sekhar, "Exploring frequency control capability of a PV system in a hybrid PV-rotating machine-without storage system," *International Journal of Electrical Power & Energy Systems*, vol. 60, pp. 258-267, Sept. 2014.

[17] Y. Ma, Z. Hu, and Y. Song, "Hour-ahead optimization strategy for shared energy storage of renewable energy power stations to provide frequency regulation service," *IEEE Transactions on Sustainable Energy*, vol. 13, no. 4, pp. 2331-2342, Oct. 2022.

[18] J. Dang, J. Seuss, L. Suneja *et al*., "SOC feedback control for wind and ESS hybrid power system frequency regulation," in *Proceedings of 2012 IEEE Power Electronics and Machines in Wind Applications*. Denver, USA, Jul. 2012, pp. 16-18.

[19] M. Rayati, A. Sheikhi, A. M. Ranjbar *et al*., "Optimal equilibrium selection of price-maker agents in performance-based regulation market," *Journal of Modern Power Systems and Clean Energy*, vol. 10, no. 1, pp. 204-212, Jan. 2022.

[20] K. Li, H. Guo, X. Fang *et al*., "Market mechanism design of inertia and primary frequency response with consideration of energy market," *IEEE Transactions on Power Systems*, vol. 38, no. 6, pp. 5701-5713, Nov. 2023.

[21] J. Wang, H. Zhong, Q. Xia *et al*., "Robust bidding strategy for microgrids in joint energy, reserve and regulation markets," in *Proceedings of 2017 IEEE PES General Meeting*, Chicago, USA, Jan. 2018, pp. 1-5.

[22] J. Zhong, L. He, C. Li *et al*., "Coordinated control for large-scale EV charging facilities and energy storage devices participating in frequency regulation," *Applied Energy*, vol. 123, pp. 253-262, Jun. 2014.

[23] R. Zhang, T. Jiang, F. Li *et al*., "Coordinated bidding strategy of wind farms and power-to-gas facilities using a cooperative game approach," *IEEE Transactions on Sustainable Energy*, vol. 11, no. 4, pp. 2545-2555, Oct. 2020.

[24] Y. Shi, B. Xu, D. Wang *et al*., "Using battery storage for peak shaving and frequency regulation: joint optimization for superlinear gains," *IEEE Transactions on Power Systems*, vol. 33, no. 3, pp. 2882-2894,

May 2018.
[25] M. K. Al-Saadi, P. C. K. Luk, and W. Fei, "Impact of unit commitment on the optimal operation of hybrid microgrids," in *Proceedings of 2016 UKACC 11th International Conference on Control*, Belfast, UK, Nov. 2016, pp. 1-5.
[26] Jiangsu Regulatory Office of the National Energy Administration. (2020, May). Trading rules for Jiangsu electric power auxiliary services (frequency modulation) market (trial). [Online]. Available: http://jsb.nea. gov. cn/eWebEditor/webpic/2020111010736764. pdf? eqid=ad928680000226d9000000026434ba28
[27] G. Li, X. Li, B. Jing *et al*., "Multi-dimensional time series simulation of large-scale photovoltaic power plant output based on hourly clear sky index," *Power System Technology*, vol. 44, no. 9, pp. 3254-3262, Sept. 2020.
[28] W. Yin, Z. Zhu, B. Kirkulak-Uludag *et al*., "The determinants of green credit and its impact on the performance of Chinese banks," *Journal of Cleaner Production*, vol. 286, p. 124991, Mar. 2021.

Jing Bian received the B.S., M.S., and Ph.D degrees in electrical engineering from Northeast Electric Power University, Jilin, China, in 2015, 2018, and 2021, respectively. His research interests include optimal operation of power system and flexible DC transmission.

Yuheng Song received the B.S. degree in electrical engineering from Northeast Electric Power University, Jilin, China, in 2019, where he is currently pursuing the Ph.D. degree. His research interests include optimal operation of power system and flexible DC transmission.

Chen Ding received the M.S. degree in electrical engineering from Northeast Electric Power University, Jilin, China, in 2023. Her research interests include optimal operation of power system and electricity market.

Jianing Cheng received the B.E. degree from Northeast Electric Power University, Jilin, China, in 2023. His research interests include renewable energy market and electricity market.

Shiqiang Li received the B.S. degree in electronic information engineering and the M.S. degree in information and communication engineering from Northeast Electric Power University, Jilin, China, in 2019 and 2022, respectively, where he is currently pursuing the Ph.D. degree in electrical engineering. His research interests include optimization, operation, and control of renewable generation, compressed sensing theory, and fault location in DC distribution network.

Guoqing Li received the B.S. and M.S. degrees in electrical engineering from Northeast Electric Power University, Jilin, China, in 1984 and 1988, respectively, and the Ph.D. in electrical engineering from Tianjin University, Tianjin, China, in 1998. He is a Professor at the Department of Electrical Engineering, Northeast Electric Power University. His research interests include security and stability analysis of power systems.